Combining Nanoliposomal Ceramide with Sorafenib Synergistically Inhibits Melanoma and Breast Cancer Cell Survival to Decrease Tumor Development

Melissa A. Tran,[1] Charles D. Smith,[6] Mark Kester,[1,4] and Gavin P. Robertson[1,2,3,4,5]

Abstract

Purpose: Deregulation of phosphatidylinositol 3-kinase/Akt and Ras/Raf/mitogen-activated protein kinase/extracellular signal-regulated kinase kinase/extracellular signal-regulated kinase pathways occurs in melanoma and breast cancer, deregulating normal cellular apoptosis and proliferation. Therapeutic cocktails simultaneously targeting these pathways could promote synergistically acting tumor inhibition. However, agents with manageable toxicity and mechanistic basis for synergy need identification. The purpose of this study is to evaluate the preclinical therapeutic efficacy and associated toxicity of combining sorafenib with nanoliposomal ceramide.

Experimental Design: Effects of sorafenib and nanoliposomal ceramide as single and combinatorial agents were examined on cultured cells using 3-(4,5-dimethylthiazol-2-yl)-5-(3-carboxymethoxyphenyl)-2-(4-sulfophenyl)-2H-tetrazolium salt assays and CalcuSyn software used to assess synergistic or additive inhibition. Western blotting measured cooperative effects on signaling pathways. Rates of proliferation, apoptosis, and angiogenesis were measured in size- and time-matched tumors to identify mechanistic basis for inhibition. Toxicity was evaluated measuring animal weight, blood toxicity parameters, and changes in liver histology.

Results: Sorafenib and nanoliposomal ceramide synergistically inhibited cultured cells by cooperatively targeting mitogen-activated protein kinase and phosphatidylinositol 3-kinase signaling. A 1- to 2-fold increase in cellular apoptosis and 3- to 4-fold decrease in cellular proliferation were observed following combination treatment compared with single agents, which caused synergistically acting inhibition. *In vivo*, an ~30% increase in tumor inhibition compared with sorafenib treatment alone and an ~58% reduction in tumor size compared with nanoliposomal ceramide monotherapy occurred by doubling apoptosis rates with negligible systemic toxicity.

Conclusions: This study shows that nanoliposomal ceramide enhances effectiveness of sorafenib causing synergistic inhibition. Thus, a foundation is established for clinical trials evaluating the efficacy of combining sorafenib with nanoliposomal ceramide for treatment of cancers.

Although novel cancer therapies are continually being developed, a cure has remained elusive for many advanced-stage solid tumor cancers. This has led to investigation of strategies simultaneously inhibiting the action of multiple targets or pathways to regulate processes promoting tumor development. These include concurrently targeting proteins or pathways regulating apoptotic resistance, proliferation, angiogenesis, cellular proliferation, tissue invasion, or metastasis (1). However, success requires identification of agents that, when combined, lead to synergistic tumor inhibition without significant systemic toxicity.

Both melanoma and breast cancer have deregulation of the phosphatidylinositol 3-kinase (PI3K)/Akt and Ras/Raf/mitogen-activated protein kinase (MAPK)/extracellular signal-regulated kinase (ERK) kinase (MEK)/ERK pathways, which regulate apoptosis and cellular proliferation, respectively (2, 3). Thus, a cocktail of agents targeting these pathways could have significant therapeutic potential by simultaneously increasing cellular apoptosis and/or decreasing proliferation in a cooperative manner. However, agents synergistically targeting these pathways with minimal associated toxicity need to be identified and the underlying mechanistic basis for synergy validated in preclinical animal models.

The MAPK signaling cascade relays an ordered series of consecutive phosphorylation events from cell surface, via Ras, Raf, MEK, and ERK, to nucleus (4, 5). In ~60% of melanomas, activation occurs through mutation of B-Raf (T1799A), an intermediate protein in the signaling pathway, resulting in

Authors' Affiliations: Departments of [1]Pharmacology, [2]Pathology, and [3]Dermatology, Pennsylvania State University College of Medicine; [4]Penn State Melanoma Therapeutics Program; [5]Foreman Foundation for Melanoma Research, Hershey, Pennsylvania; and [6]Department of Pharmaceutical Sciences, Medical University of South Carolina, Charleston, South Carolina

Received 11/12/07; revised 1/22/08; accepted 2/15/08.

Grant support: Melanoma Research Foundation, American Cancer Society grant RSG-04-053-01-GMC, Foreman Foundation for Melanoma Research, Elsa U. Pardee Foundation, and State of Pennsylvania Non-formulary Tobacco Settlement Funds.

The costs of publication of this article were defrayed in part by the payment of page charges. This article must therefore be hereby marked *advertisement* in accordance with 18 U.S.C. Section 1734 solely to indicate this fact.

Requests for reprints: Gavin P. Robertson, Department of Pharmacology-R130, Pennsylvania State University College of Medicine, 500 University Drive, Hershey, PA 17033. Phone: 717-531-8098; Fax: 717-531-5013; E-mail: gprobertson@psu.edu.

doi:10.1158/1078-0432.CCR-07-4881

kinase activity 10.7 times higher than occurs in normal cells (6–9). The MAPK pathway is similarly activated in breast cancer cells with ~100% having pathway activation due in part to aberrant Ras or Raf-1 activity (10). In melanoma and breast cancer animal models, inhibition of the MAPK signaling cascade significantly retards tumorigenesis, making targeting this pathway an important component of a combinatorial therapeutic approach (11–14).

The MAPK signaling cascade has been inhibited in both melanomas and breast cancer preclinical models using sorafenib (BAY 43-9006), which is a nonspecific Raf kinase inhibitor (14, 15). In animal models, sorafenib effectively reduces melanoma, breast cancer, colon, and lung cancer development (11, 14). However, clinical efficacy has been shown for only renal cell carcinoma, where it is approved for clinical use (16, 17). To improve efficacy for other cancers, novel agent combinations are being evaluated in which sorafenib is combined with agents to identify therapeutic cocktails that simultaneously inhibit pathways resulting in synergy and greater tumor-inhibitory efficacy.

A second pathway deregulated in a large proportion of melanoma and breast cancer is the PI3K/Akt signaling cascade. This pathway relays signals through an ordered series of consecutive phosphorylation events from cell surface, via PI3K and Akt, to a wide range of downstream targets, some of which regulate cellular apoptosis (FOXO, GSK-3, BAD, PRAS40, and MDM2; refs. 18, 19). Deregulation of the apoptotic pathway promotes chemoresistance, reducing the effectiveness of chemotherapeutic agents (1, 20). The PI3K/Akt pathway is activated in ~70% of melanomas and in 25% to 55% of breast cancers (3, 21). In melanoma and breast cancer animal models, inhibition of PI3K/Akt signaling retards tumorigenesis by restoring the apoptotic sensitivity of cancer cells to environmental stimuli and chemotherapeutic agents triggering apoptosis, making targeting this pathway an important component of a combinatorial therapeutic approach (11–13, 21–23).

Although inhibitors of the PI3K/Akt pathway, such as API-2 and rapamycin, have been developed and had varying clinical efficacy, potentially more effective agents with less toxicity are being developed (24). The use of ceramide to inhibit Akt signaling is a novel approach under preclinical evaluation.[7] Ceramide targets the PI3K/Akt pathway through dephosphorylation of Akt, leading to increased tumor cell apoptosis and in combination with other chemotherapeutics can enhance cancer cell death (22, 23, 25–31). An obstacle that has limited clinical use of ceramide is its hydrophobicity, which has been overcome by packaging it into a nanoliposomal formulation for systemic delivery (22, 23, 29, 30). Nanoliposomal ceramide can reduce melanoma and breast cancer development by targeting PI3K/Akt signaling (22, 23, 29, 30, 32). It is possible that nanoliposomal ceramide could be combined with other drugs into a therapeutic cocktail that simultaneously inhibits multiple pathways leading to synergistic tumor inhibition.

In this study, combining sorafenib and nanoliposomal ceramide has been found to more effectively inhibit melanoma and breast tumor development than either agent alone. By therapeutically targeting the MAPK and PI3K/Akt pathways, these agents cause a 1- to 2-fold increase in cellular apoptosis and 3- to 4-fold decrease in proliferation compared with single agents. An ~30% reduction in tumor development compared with sorafenib alone and ~58% decrease in tumor size compared with nanoliposomal ceramide monotherapy were observed with the combination treatment. Thus, these results lay the groundwork for clinical trials testing the safety and efficacy of combining sorafenib with nanoliposomal ceramide for more effectively treating melanoma and breast cancer patients.

Materials and Methods

Cell line culture conditions and B-Raf mutational status. The human melanoma cell lines UACC 903 and 1205 Lu and human fibroblast cells FF2441 were maintained in DMEM (Invitrogen) supplemented with 10% fetal bovine serum (Hyclone). The human breast cancer cell line MDA-MB-231 was maintained in RPMI 1640 (Mediatech) supplemented with 10% fetal bovine serum. Melan-A cells are mouse melanocytes that were grown in RPMI 1640 supplemented with 10% fetal bovine serum, 2 mmol/L L-glutamine (Mediatech), and 200 nmol/L 12-*O*-tetradecanoylphorbol-13-acetate (Sigma-Aldrich). The presence of the (T1799A) *B-RAF* mutation in UACC 903 and 1205 Lu cells has been reported previously (11). MDA-MB-231 contains mutations in both KRas and B-Raf leading to MAPK pathway activation (14).

Preparation of nanoliposomal ceramide. Pegylated nanoliposomes (80 ± 15 nm in size) that contain 30 mol% ceramide were prepared as described previously with lipids 1,2-distearoyl-*sn*-glycero-3-phosphocholine, 1,2-dioleoyl-*sn*-glycero-3-phosphoethanolamine, *N*-hexanoyl-D-*erythro*-sphingosine (C_6), 1,2-distearoyl-*sn*-glycero-3-phosphoethanolamine-*N*-[methoxy polyethylene glycol-2000], and *N*-octanoyl-sphingosine-1-[succinyl(methoxy polyethylene glycol-750)] (PEG(750)-C_8) combined in chloroform at a molar ratio of 3.75:1.75:3:0.75:0.75 (22, 23). Combined lipids were dried under nitrogen gas and resuspended in 0.9% sterile NaCl at 60°C. Following rehydration, resulting solution was sonicated for 5 min followed by extrusion through a 100-nm polycarbonate membrane using the Avanti Mini Extruder (Avanti Polar Lipids). Ghost liposomes were prepared in a similar manner excluding *N*-hexanoyl-D-*erythro*-sphingosine (C_6).

Cytotoxicity of sorafenib and nanoliposomal ceramide in cultured cells. Sorafenib [BAY 43-9006; *N*-(3-trifluoromethyl-4-chlorophenyl)-*N*′-(4-[2-methylcarbamoyl pyridin-4-yl]ocyphenyl)urea] was prepared as described previously (11). Cytotoxicity of sorafenib and nanoliposomal ceramide alone in fibroblast, breast cancer, and melanoma cells was measured by plating 5×10^3 cells into 96-well plates followed by growth for 48 h in a humidified 37°C cell culture incubator. Next, cells were treated with sorafenib, DMSO, nanoliposomal ceramide, or ghost liposomes for 24 h in 2.5% serum medium (sorafenib: 0.5, 1.0, 1.5, and 2.0 μmol/L; nanoliposomal ceramide: 3.125, 6.25, 12.5, and 25 μmol/L). For combination agent studies, 5×10^3 cells were plated in 96-well plates, allowed to recover for 48 h, and treated with ghost liposome + DMSO, ghost liposome + sorafenib, nanoliposomal ceramide + DMSO, or nanoliposomal ceramide + sorafenib for 24 h in 2.5% serum medium. After 24 h, cytotoxicity was measured using the CellTiter 96 Aqueous Non-Radioactive Cell Proliferation Assay (Promega).

Western blot analysis. For Western blot analysis, cell lysates were harvested in Petri dishes by addition of lysis buffer containing 50 mmol/L HEPES (pH 7.5), 150 mmol/L NaCl, 10 mmol/L EDTA, 10% glycerol, 1% Triton X-100, 1 mmol/L sodium orthovanadate, 0.1 mmol/L sodium molybdate, 1 mmol/L phenylmethylsulfonyl

[7] Penn State Research Foundation has licensed ceramide liposomes to TRACON Pharmaceuticals, Inc.

fluoride, 20 μg/mL aprotinin, and 5 μg/mL leupeptin. Whole-cell lysates were centrifuged (≥10,000 × *g*) for 10 min at 4°C to remove cell debris. Protein concentrations were quantitated using the bicinchoninic acid assay from Pierce, and 30 μg of lysate per lane were loaded onto a NuPAGE gel (Life Technologies, Inc.). Following electrophoresis, samples were transferred to polyvinylidene difluoride membrane (Pall Co.). Blots were probed with antibodies according to each supplier's recommendations: MEK1/2, phosphorylated MEK (pMEK), Akt, and phosphorylated Akt (pAkt) from Cell Signaling Technology; antibodies to B-Raf, ERK2, cyclin D1, and p27 from Santa Cruz Biotechnology. Secondary antibodies were conjugated with horseradish peroxidase and obtained from Santa Cruz Biotechnology. Immunoblots were visualized using the enhanced chemiluminescence detection system (Amersham Pharmacia Biotech).

Caspase-3/7 detection. Levels of caspase-3/7 activity in cells were measured by plating 5×10^3 cells per well in 96-well plates and grown for 48 h in a humidified 37°C cell culture incubator followed by addition of ghost liposome + DMSO vehicle, ghost liposome + sorafenib, nanoliposomal ceramide + DMSO vehicle, or nanoliposomal ceramide + sorafenib in 2.5% serum-containing medium. After 24 h, levels of caspase-3/7 activity were measured using the Apo-ONE Homogeneous Caspase-3/7 Assay (Promega). The kit measures caspase-3/7 activity by quantifying cleavage of rhodamine 110, bis-(*N*-CBZ-L-aspartyl-L-glutamyl-L-valyl-L-aspartic acid amide) due to enzymatically active caspase-3/7. Plates were read using a fluorescence plate reader with an excitation of 485 nm and an emission of 530 nm.

Proliferation of cultured cells. To quantify effects of sorafenib and nanoliposomal ceramide on cell proliferation, 5×10^3 cells per well were plated in 96-well plates and grown for 48 h in a humidified 37°C cell culture incubator followed by addition of ghost liposome + DMSO vehicle, ghost liposome + sorafenib, nanoliposomal ceramide + DMSO, or nanoliposomal ceramide + sorafenib in medium containing 2.5% serum. After 24 h, bromodeoxyuridine labeling solution from the Cell Proliferation Biotrak ELISA System was added for 16 h, after which samples were processed according to the kit instructions and absorbance was read at 450 nm (Amersham Pharmacia Biotech).

Sorafenib and nanoliposomal ceramide studies in animals. Tumor-inhibitory effect of sorafenib and nanoliposomal ceramide was measured by s.c. injection of 5×10^6 UACC 903 cells or 10×10^6 MDA-MB-231 cells into nude mice (four mice per group, two tumors per mouse, with two replicates). After 6 d, when a small vascularized tumor (50-100 mm^3) had developed, mice received an i.p. injection on alternate days consisting of 50 μL of vehicle (DMSO), or sorafenib at concentrations of 50 mg/kg body weight for UACC 903 cells and 25 mg/kg body weight for MDA-MB-231 cells (11, 14). Nanoliposomal ceramide or ghost liposomes were delivered i.v. daily at a dose of 36 mg/kg ceramide. The mechanism by which sorafenib and nanoliposomal ceramide decreased tumorigenicity was identified by s.c. injection of 5×10^6 UACC 903 cells followed at day 6 by i.p. injection every 2 d with 50 mg/kg sorafenib and every day injections i.v. of nanoliposomal ceramide. Control groups included DMSO + ghost liposome, sorafenib + ghost liposome, and DMSO + nanoliposomal ceramide at the same dosing schedule. At each time point, tumors of the same size developing in parallel from mice treated with DMSO vehicle or drug were harvested for analysis of cell proliferation, apoptosis, and vascular development (11).

Toxicity analysis. To determine whether the combination of nanoliposomal ceramide and sorafenib was toxic to animals, Swiss Webster mice were injected daily with nanoliposomal ceramide (36 mg/kg) or ghost liposomes and on alternate days with sorafenib (50 mg/kg) or DMSO. The combination of nanoliposomal ceramide and sorafenib was compared with control groups of ghost liposome + DMSO, ghost liposome + sorafenib, and nanoliposomal ceramide + DMSO at the same dosing schedule. Each group of five mice was weighed on alternate days, and after 20 d of treatment, the mice were sacrificed, livers were removed for formalin fixation and paraffin embedding for H&E examination, and blood was collected for analysis to determine changes in serum glutamic oxaloacetic transaminase, serum glutamic pyruvic transaminase, glucose, and alkaline phosphatase. Values represent the average of at least four samples ± SE depicted as percentage of ghost liposome + DMSO–treated cells.

Apoptosis, cell proliferation, and vessel density measurements in tumors. Apoptosis measurements on formalin-fixed, paraffin-embedded tumor sections were undertaken using the terminal deoxynucleotidyl transferase–mediated dUTP nick end labeling (TUNEL) TMR Red Apoptosis kit from Roche (11, 21). Cell proliferation rates in formalin-fixed tumor sections were measured using Ki-67 staining (33). The number of positive cells per field (1,392 × 1,040 pixels) was quantified from a minimum of four fields per tumor for both TUNEL and Ki-67 staining. Vessel density was quantified using a purified FITC-conjugated CD31 (platelet endothelial cell adhesion molecule 1) antibody (PharMingen). Frozen sections were fixed in acetone at -20°C for 5 min and rinsed in PBS. Sections were blocked in 1% bovine serum albumin for 30 min followed by incubation with primary antibody overnight at 4°C. Sections were then rinsed with PBS and mounted using a 4′,6-diamidino-2-phenylindole–containing mountant (Vector Laboratories, Inc.). Proportional area of the tumors occupied by vessels over total area was calculated using the IPLab imaging software program (BD Biosciences Bioimaging). For all tumor analyses, a minimum of three different tumors with four to six fields per tumor was analyzed and results were represented as the average ± SE.

Statistical analysis. One-way or two-way ANOVA followed by the appropriate post hoc test (Tukey's or Bonferroni) was used to establish whether significant differences existed between groups. Differences were considered significant at $P < 0.05$. The nature of the interaction between sorafenib and nanoliposomal ceramide was calculated using the Chou-Talalay method for determining the combination index using CalcuSyn software (Biosoft; ref. 34). Based on this approach, combination index values <0.9 are considered synergistic, >1.1 are antagonistic, and values 0.9 to 1.1 are nearly additive (34).

Results

Sorafenib inhibits cancer cell viability. Because sorafenib reduces cancer cell viability by decreasing MAPK pathway signaling, its growth-inhibitory potential was initially confirmed on melanoma and breast cancer cells (11, 14). Melanoma (UACC 903 and 1205 Lu) or breast cancer (MDA-MB-231) cell lines were plated in 96-well plates and treated with increasing concentrations of sorafenib (0.5, 1.0, 1.5, and 2.0 μmol/L) or DMSO vehicle in reduced serum culture medium. Following 24 h of treatment, cell viability was assessed using the 3-(4,5-dimethylthiazol-2-yl)-5-(3-carboxymethoxyphenyl)-2-(4-sulfophenyl)-2H-tetrazolium salt assay, showing significant reductions in both melanoma and breast cancer cell viability compared with DMSO control–treated cells (Fig. 1A). Similarly, sorafenib inhibited cultured normal human fibroblasts (FF2441), although the agent is well tolerated in patients with manageable toxicity (Fig. 1A; refs. 16, 17, 35).

The effect of sorafenib (0.5, 1.0, 1.5, and 2.0 μmol/L) on MAPK pathway signaling was examined by Western blotting and compared with DMSO vehicle–treated cells. Following 24 and 48 h of sorafenib exposure, pMEK and cyclin D1 levels decreased, whereas p27 protein increased in both breast and melanoma cells (Fig. 1B and C). This pattern is indicative of nonproliferative cells following inhibition of MAPK signaling (2). In contrast, pAkt levels were slightly reduced in UACC 903 cells (Fig. 1B) and were marginally elevated in MDA-MB-231

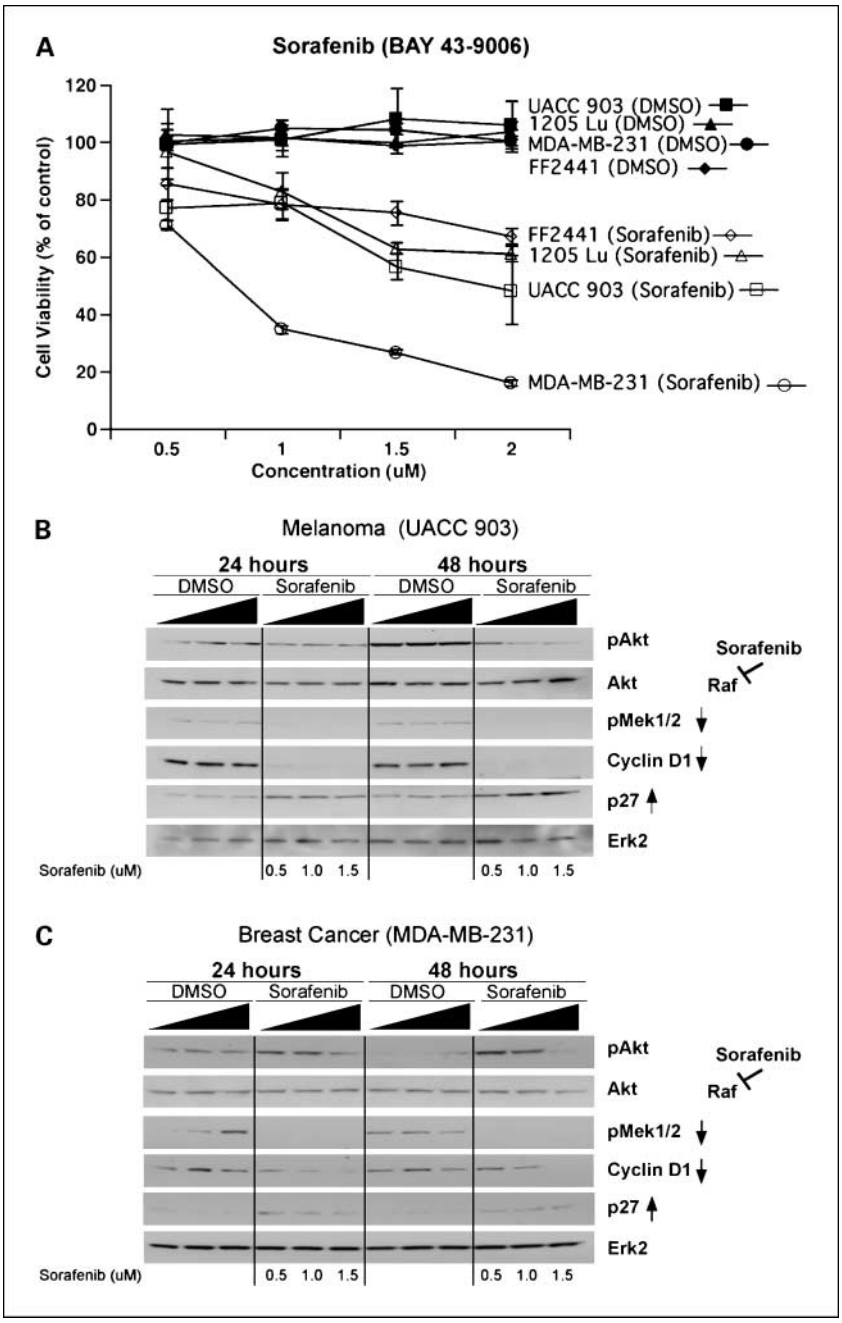

Fig. 1. Sorafenib decreases cancer cell viability through down-regulation of MAPK pathway signaling. *A,* treatment of melanoma (UACC 903 and 1205 Lu), breast cancer (MDA-MB-231), or fibroblast (FF2441) cells with increasing concentrations of sorafenib (0.5, 1.0, 1.5, and 2.0 μmol/L) but not control DMSO led to a dose-dependent decrease in cell viability following 24 h of exposure. *B* and *C,* treatment of melanoma (UACC 903) or breast cancer (MDA-MB-231) cells with sorafenib (0.5, 1.0, and 1.5 μmol/L) but not control DMSO decreased levels of pMEK and cyclin D1, with corresponding increases in p27 following 24 and 48 h of exposure. ERK2 served as a control for protein loading.

cells (Fig. 1C) except at the highest concentrations of drug used. Sorafenib was originally identified as a Raf kinase inhibitor; however, dependent on the dose and time following treatment, it can affect Akt activity (36). Because no consistent trend was observed in both cell lines in this study and the changes were marginal, effect on Akt activity was considered negligible especially when compared with effects on MAPK signaling. Thus, sorafenib decreased viability of melanoma and breast cancer cells mediated through decreased MAPK cascade activity and had a negligible inconsistent effect on Akt pathway signaling.

Nanoliposomal ceramide inhibits cell viability. To validate earlier reports, showing that nanoliposomal ceramide inhibits cell survival mediated through decreased Akt activity, melanoma (UACC 903 and 1205 Lu) and breast cancer (MDA-MB-231) cells were exposed to nanoliposomal ceramide and compared with control human fibroblasts (FF2441) as well as melanocytes (melan-A; refs. 22, 23). Cells were plated in 96-well plates and treated with increasing concentrations of nanoliposomal ceramide (3.125, 6.25, 12.5, and 25 μmol/L) or ghost liposomes lacking ceramide in reduced serum medium, and cell viability was quantified 24 h later. Nanoliposomal ceramide decreased cell viability in UACC 903, 1205 Lu (data not shown), and MDA-MB-231 cells while having minimal effect on fibroblasts (FF2441) and melanocytes (melan-A; data not shown Fig. 2A). Results were consistent with prior reports showing that ceramide had negligible effect on normal breast cells (22).

To examine the effect of nanoliposomal ceramide on PI3K/Akt pathway signaling and validate prior reports that nanoliposomal ceramide decreases Akt activity, UACC 903 or MDA-MB-231 cells were treated with increasing concentrations of nanoliposomal ceramide (12.5, 25.0, and 50.0 μmol/L or 1.5, 3.0, and 6.0 μmol/L, respectively) or ghost liposomes and protein lysates were isolated 24 and 48 h later for Western blot analysis (23). Nanoliposomal ceramide consistently reduced pAkt levels at 24 and 48 h compared with DMSO control–treated cells. In contrast, compared with DMSO-treated cells, pMEK and cyclin D1 remained unchanged or decreased only after 48 h of exposure at the highest concentrations examined when cells were dying due to the inhibitory action of the drug on its target. Thus, results suggested that ceramide had a negligible effect on MAPK signaling (Fig. 2B and C). These results indicate that nanoliposomal ceramide can target cancer cells by inhibiting PI3K/Akt pathway activity.

Sorafenib and nanoliposomal ceramide cooperate to inhibit melanoma and breast cancer cell growth. Because sorafenib and nanoliposomal ceramide are effective inhibitors of melanoma and breast cancer cells, effectiveness of combining agents for

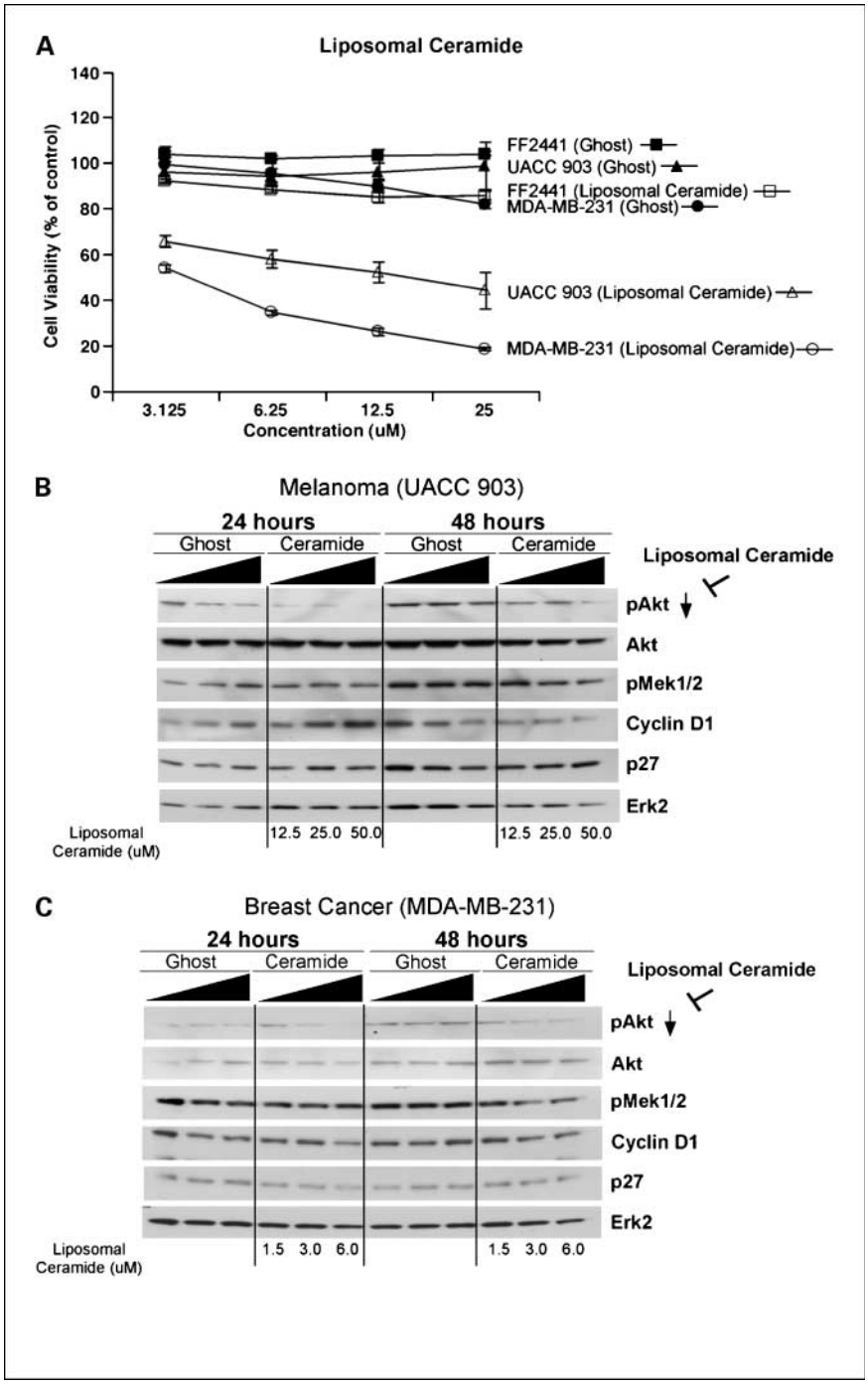

Fig. 2. Nanoliposomal ceramide inhibits cancer cell viability by decreasing Akt activity. *A,* treatment of melanoma (UACC 903) or breast cancer (MDA-MB-231) cells with increasing concentrations of nanoliposomal ceramide (3.12, 6.25, 12.5, and 25 μmol/L) but not control ghost liposomes resulted in a dose-dependent decrease in cell viability following 24 h of exposure. Similar treatment did not significantly affect control fibroblast cell survival (FF2441). *B* and *C,* treatment of melanoma (UACC 903; 12.5, 25.0, and 50.0 μmol/L) or breast cancer (MDA-MB-231; 1.5, 3.0, and 6.0 μmol/L) cell lines with nanoliposomal ceramide but not control ghost liposomes decreased levels of pAkt following 24 and 48 h of exposure. No consistent changes in levels of MAPK pathway proteins pMEK, cyclin D1, or p27 were observed. ERK2 served as a control for protein loading.

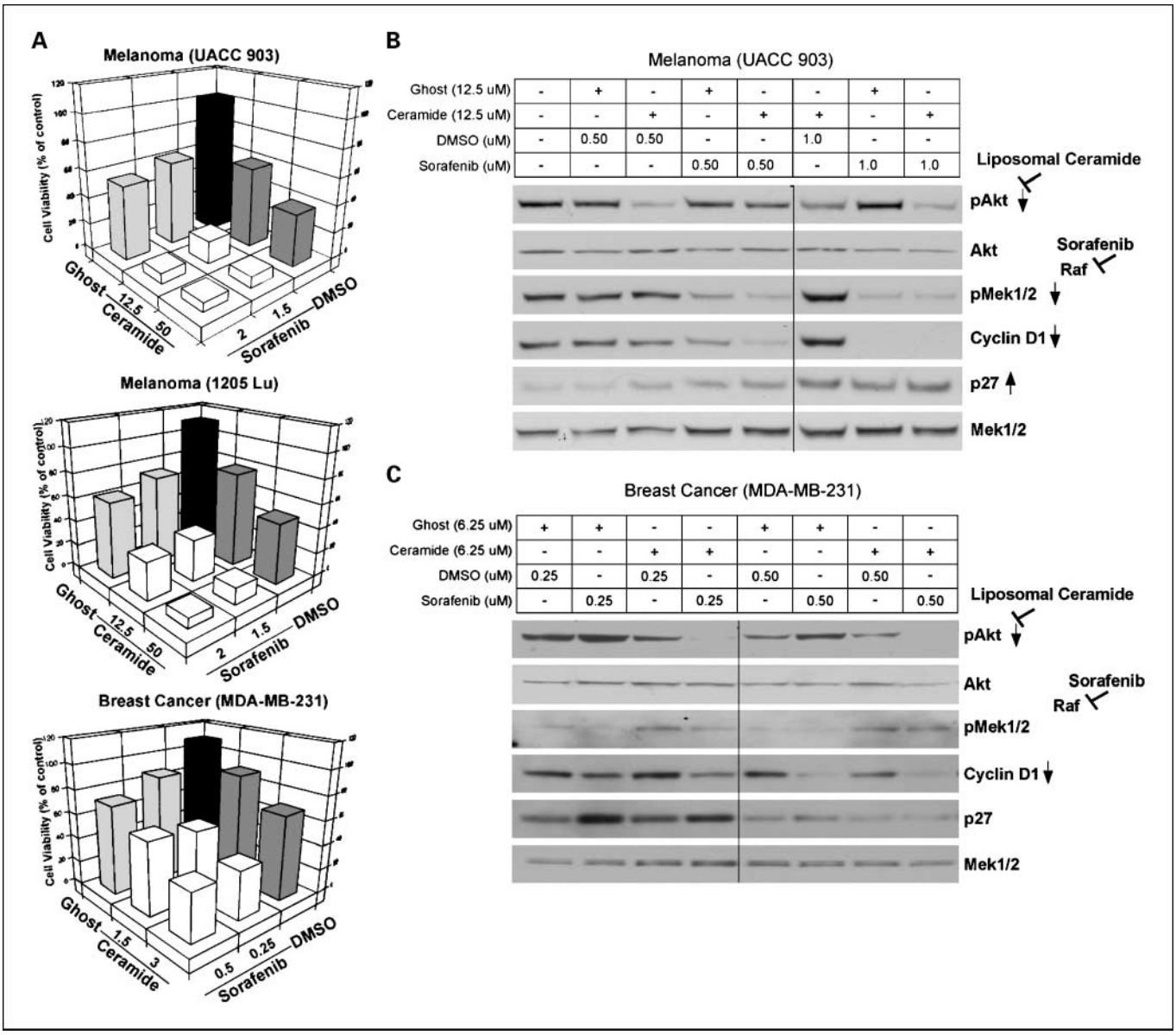

Fig. 3. Sorafenib and nanoliposomal ceramide cooperate to synergistically decrease viability of cultured cancer cells. *A,* treatment of melanoma or breast cancer with sorafenib (UACC 903 and 1205 Lu, 1.5 and 2.0 μmol/L; MDA-MB-231, 0.25 and 0.5 μmol/L) and nanoliposomal ceramide (UACC 903 and 1205 Lu, 12.5 and 50 μmol/L; MDA-MB-231, 1.5 and 3.0 μmol/L) in combination cooperates to decrease cell viability compared with single agents, control DMSO, or ghost liposome – treated cells. *B* and *C,* combined treatment using sorafenib and nanoliposomal ceramide decreased pAkt, pMEK, and cyclin D1 as well as increased p27 in both melanoma (UACC 903; *B*) and breast cancer (MDA-MB-231; *C*) cells. Compared with cells treated for 24 h with control ghost liposomes + DMSO, or monotherapies, sorafenib + nanoliposomal ceramide significantly reduced pAkt and cyclin D1 levels. MEK1/2 served as a control for protein loading.

inhibiting cell survival was evaluated. UACC 903, 1205 Lu, and MDA-MB-231 were treated with sorafenib, nanoliposomal ceramide, or sorafenib plus nanoliposomal ceramide in reduced serum medium and compared with vehicle control (DMSO or ghost liposomes; Fig. 3A). Twenty-four hours later, cell viability was measured by 3-(4,5-dimethylthiazol-2-yl)-5-(3-carboxymethoxyphenyl)-2-(4-sulfophenyl)-2H-tetrazolium salt assay, which showed a pronounced decrease in cell viability for all cell lines with combined agents compared with single treatments (Fig. 3A). Melanoma cells (UACC 903 and 1205 Lu) treated with 1.5 μmol/L sorafenib showed a 27% to 38% reduction in cell viability, whereas cells treated with 12.5 μmol/L nanoliposomal ceramide exhibited a 23% to 41% reduction in viability. In comparison, combined agents decreased cell viability by 65% to 84%, which was an approximately 2- to 4-fold increase compared with single agents (Fig. 3A). Similarly, MDA-MB-231 breast cancer cells treated with 0.25 μmol/L sorafenib or 1.5 μmol/L nanoliposomal ceramide showed a 10% to 13% reduction in cell viability with single agents compared with an ~46% decrease with combined agents, which was an approximately 4- to 5-fold increase in efficacy compared with single agents. Similar inhibitory results of the agent combination were seen with normal human fibroblasts (FF2441; data not shown). Thus, combining sorafenib with nanoliposomal ceramide led to cooperative inhibition of cultured cells.

Sorafenib and nanoliposomal ceramide synergistically decrease cell viability. Because combining sorafenib and nanoliposomal ceramide caused a significant reduction in the proliferative potential of cancer cells, the combination index approach was used to determine whether agents led to additive or synergistic inhibition (34). For melanoma cell lines, combination index values were within ranges of 0.05 to 0.154 for UACC 903 and 0.321 to 0.694 for 1205 Lu, which indicate synergism between sorafenib and nanoliposomal ceramide. MDA-MB-231 results were also consistent with synergism except at 0.5 μmol/L sorafenib and 1.5 μmol/L nanoliposomal ceramide where it was additive, with values between 0.575 and 1.043. Thus, sorafenib and nanoliposomal ceramide cooperate synergistically to decrease melanoma and breast cancer cell survival.

Sorafenib and nanoliposomal ceramide cooperate to decrease PI3K/Akt and MAPK pathway signaling. To ascertain the mechanism leading to synergy between sorafenib and nanoliposomal ceramide, effects on PI3K/Akt and MAPK pathway signaling were examined using Western blot analysis. As predicted, sorafenib decreased pMEK and cyclin D1 levels with corresponding up-regulation of p27, whereas nanoliposomal ceramide decreased pAkt levels for melanoma cells (Fig. 3B). Significantly, combined sorafenib and nanoliposomal ceramide treatment enhanced reduction of pMEK, pAkt, and cyclin D1 levels, with correspondingly increased p27 compared with single-agent treatments (Fig. 3B). A similar trend was observed for breast cancer cells with enhanced reduction of pAkt and cyclin D1 levels (Fig. 3C). However, changes in pMEK1/2 and p27 levels were subtle, likely due to differential pathway signaling. Thus, simultaneous exposure of melanoma or breast cancer cells to sorafenib and nanoliposomal ceramide enhanced down-regulation of PI3K/Akt and MAPK pathway signaling.

Combining sorafenib and nanoliposomal ceramide enhanced apoptosis and cooperatively decreased cell proliferation. Because sorafenib and nanoliposomal ceramide synergistically decreased cancer cell viability, the underlying mechanism contributing to cooperative inhibition was investigated by comparing effects on apoptosis and proliferation. Following 24 h of exposure to sorafenib and/or nanoliposomal ceramide, activity of caspase-3 and caspase-7 was measured. Compared with single agents, combined sorafenib and nanoliposomal ceramide led to a statistically significant 1- to 2-fold increase in cellular apoptosis in both melanoma (Fig. 4A) and breast cancer (Fig. 4B) cells ($P < 0.05$, one-way ANOVA). Furthermore, TUNEL staining of UACC 903 cells showed a 2-fold increase of apoptosis following combined treatment compared with single agents (data not shown). Next, cellular proliferation was examined by measuring bromodeoxyuridine incorporation (Fig. 4C). Whereas single agents reduced proliferative capacity of UACC 903 melanoma cells by ~2-fold, combined agents decreased proliferation by 3- to 4-fold ($P < 0.05$, one-way ANOVA; Fig. 4C). Thus, combining sorafenib with nanoliposomal ceramide increased cellular apoptosis and decreased proliferative capacity of

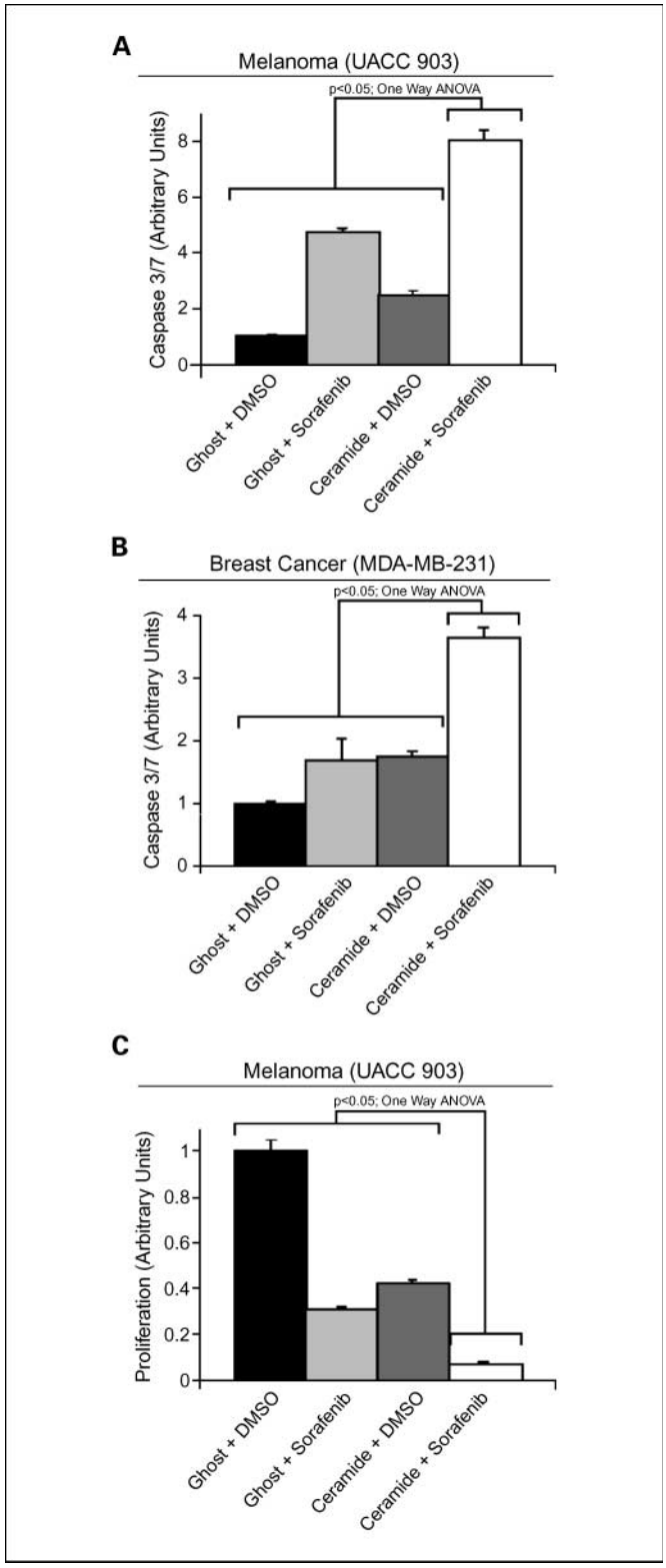

Fig. 4. Sorafenib and nanoliposomal ceramide cooperate to increase cellular apoptosis and decrease proliferation in cultured cancer cells. *A* and *B,* melanoma (UACC 903) and breast cancer (MDA-MB-231) cells treated with sorafenib [UACC 903, 1.5 μmol/L (*A*); MDA-MB-231, 0.5 μmol/L (*B*)] and nanoliposomal ceramide [UACC 903, 12.5 μmol/L (*A*); MDA-MB-231, 3.0 μmol/L (*B*)] show increased caspase-3/7 activity levels when compared with monotherapies or control ghost liposomes + DMSO – treated cells ($P < 0.05$, one-way ANOVA). *C,* melanoma (UACC 903) cells treated simultaneously with sorafenib (1.5 μmol/L) and nanoliposomal ceramide (12.5 μmol/L) show significant decrease in proliferation compared with cells treated with control ghost liposomes + DMSO vehicle, ghost liposomes + sorafenib, or nanoliposomal ceramide + DMSO ($P < 0.05$, one-way ANOVA).

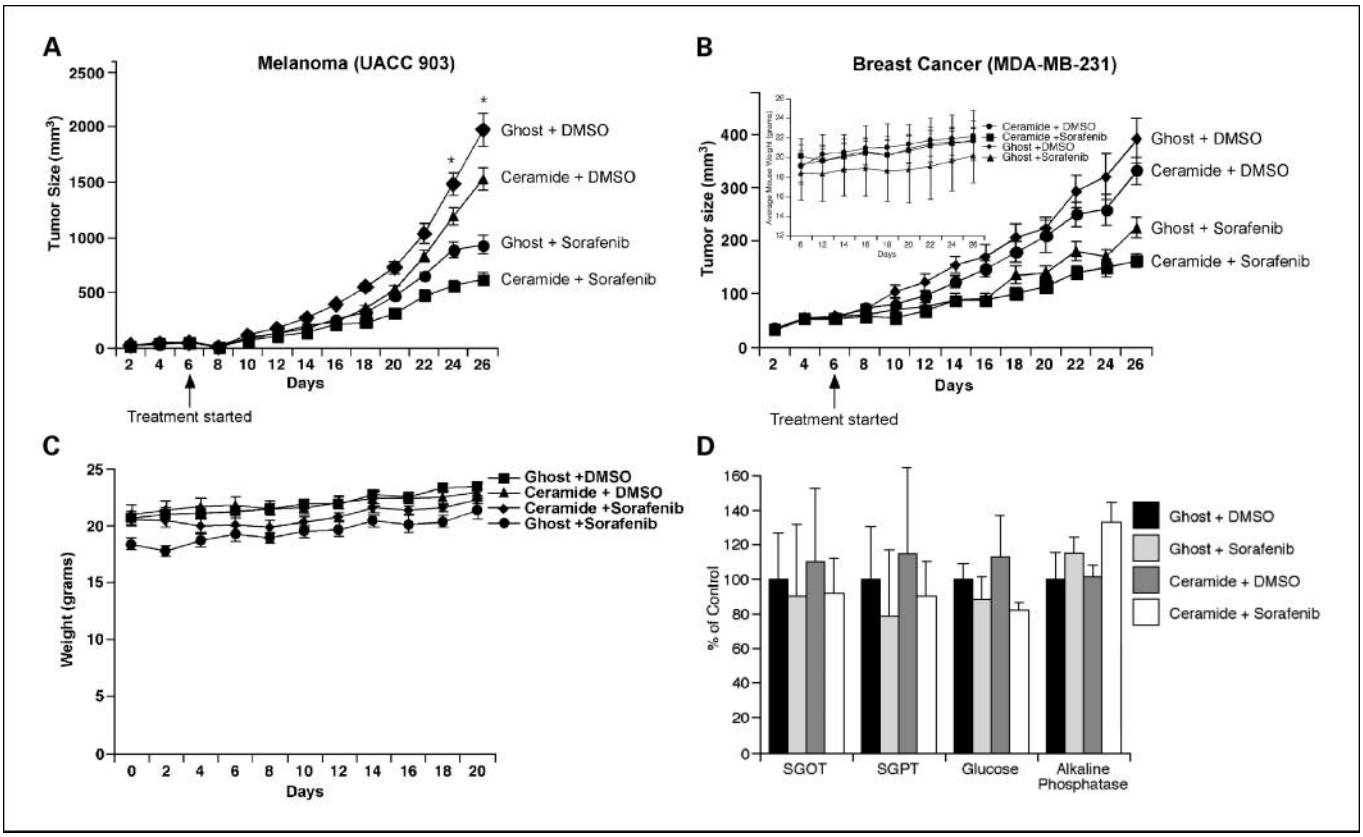

Fig. 5. Combination of sorafenib and nanoliposomal ceramide therapy cooperates to inhibit tumor development with negligible toxicity. Melanoma (UACC 903, 5×10^6; *A*) or breast cancer (MDA-MB-231, 10×10^6; *B*) cells were s.c. injected into nude mice, and after 6 d, mice were treated on alternate days with sorafenib (UACC 903, 50 mg/kg; MDA-MB-231, 25 mg/kg) or DMSO and daily with nanoliposomal ceramide (36 mg/kg) or ghost liposome. Tumors were measured with calipers on alternate days. Significant tumor inhibition occurred when using the combination sorafenib and nanoliposomal ceramide treatment (UACC 903; $P < 0.05$, two-way ANOVA). Weights of MDA-MB-231 tumor-bearing mice were measured on alternate days and no significant differences between groups were observed ($P > 0.05$, two-way ANOVA). *C,* weights of Swiss Webster mice treated daily with nanoliposomal ceramide (36 mg/kg) or ghost liposomes and on alternate days with sorafenib (50 mg/kg) or DMSO were measured to establish toxicity. No significant loss of weight was detected ($P > 0.05$, two-way ANOVA). *D,* blood from Swiss Webster mice under the various treatment regimens was collected and analyzed for changes in serum glutamic oxaloacetic transaminase (*SGOT*), serum glutamic pyruvic transaminase (*SGPT*), glucose, and alkaline phosphatase to identify any organ-related toxicity. No significant changes in blood toxicity parameters were seen between groups ($P > 0.05$, two-way ANOVA).

cultured cancer cells, suggesting enhanced efficacy for inhibiting tumor development.

Combining sorafenib and nanoliposomal ceramide enhanced tumor inhibition. Because combining agents was more effective at inhibiting cultured cancer cells, effect on tumor development was examined next. UACC 903 melanoma or MDA-MB-231 breast cancer cells were injected s.c. into nude mice, and 6 days later, when a vascularized tumor had developed, mice were randomly placed into groups and treated with ghost liposome + DMSO, ghost liposome + sorafenib, nanoliposomal ceramide + DMSO, or nanoliposomal ceramide + sorafenib. Sorafenib was given on alternate days at 50 mg/kg body weight for UACC 903 and 25 mg/kg body weight for MDA-MB-231 (11, 14). Nanoliposomal ceramide was given i.v. into the lateral tail vein daily at 36 mg/kg body weight, which is a submaximal dose previously shown to maintain optimal ceramide levels at the tumor site above the calculated IC_{50} value necessary for apoptosis (22). Tumors were measured with calipers and animals were weighed on alternate days to ascertain possible systemic toxicity. Although sorafenib or nanoliposomal ceramide treatments reduced tumor growth, this effect was enhanced when agents were combined for melanoma (Fig. 5A) and breast cancer (Fig. 5B). A statistically significant reduction of UACC 903 melanoma tumor development was observed in mice receiving the combination of agents compared with individual ones at days 24 and 26 ($P < 0.05$, two-way ANOVA). Furthermore, no significant weight loss was seen for any treatment regimen ($P > 0.05$, two-way ANOVA; Fig. 5B). Thus, combining nanoliposomal ceramide with sorafenib more effectively reduced melanoma and breast cancer development that either agent alone.

Combined sorafenib and nanoliposomal ceramide did not cause systemic toxicity. To further confirm that sorafenib and nanoliposomal ceramide did not induce systemic toxicity compared with control-treated mice, Swiss Webster mice were treated i.v. daily with nanoliposomal ceramide (36 mg/kg) or ghost liposomes and on alternate days i.p. with sorafenib (50 mg/kg) or DMSO. No significant weight loss was observed for any group ($P > 0.05$, two-way ANOVA; Fig. 5C). After 20 days of treatment, mice were sacrificed and blood was collected for major organ toxicity assessment. Levels of serum glutamic oxaloacetic transaminase, serum glutamic pyruvic transaminase, glucose, and alkaline phosphatase were measured for all groups, and no significant differences were observed between any groups ($P > 0.05$, one-way ANOVA; Fig. 5D). In addition, microscopic analysis of H&E-stained liver sections from

experimental and control mice showed no significant morphologic differences (data not shown). Thus, no discernible toxicity was detected in animals treated with nanoliposomal ceramide and sorafenib compared with controls.

Combining sorafenib with nanoliposomal ceramide enhanced tumor cell apoptosis. To establish the mechanism leading to tumor inhibition following the combined treatment, size- and time-matched tumors were harvested at days 9 and 11 and compared with single-agent treatments for changes in apoptosis, proliferation, and vascular development. The number of TUNEL-positive apoptotic cells increased significantly for the combined treatment group compared with monotherapies or vehicle-treated control tumors ($P < 0.05$, two-way ANOVA; Fig. 6A). In contrast, no significant changes in proliferation (Fig. 6B) or vascular development (Fig. 6C) compared with single-agent treatments were observed ($P > 0.05$, two-way ANOVA). The sorafenib and nanoliposomal ceramide combination significantly affected cellular apoptosis, which doubled, leading to tumor reduction compared with monotherapies. Thus, combining sorafenib with nanoliposomal ceramide enhanced tumor cell apoptosis, thereby promoting cooperative tumor inhibition.

Discussion

Melanoma and breast cancer require more effective treatment options for advanced-stage patients. One possibility involves simultaneously targeting multiple pathways leading to tumorigenesis. Both animal studies and clinical trials show that coadministration of therapeutic agents can be more beneficial than monotherapies (36–40). A case in point is sorafenib where clinical trials show that this agent can be effective in renal cell cancer patients with few minor clinically manageable side effects extending life by ~12 weeks (16, 17, 35, 39, 41–44). However, sorafenib is less effective for treating other types of cancer, including melanoma and breast cancer, which is driving the search for agents that can be combined with sorafenib to enhance its clinical efficacy (16, 35, 39, 41, 43, 44).

Combining sorafenib with rottlerin, a protein kinase C inhibitor, which causes synergistic inhibition of cell proliferation and increased apoptosis in glioma cells, shows a solid mechanistic basis for combining these agents in the clinic (36). Furthermore, radiation followed by sorafenib treatment can significantly decrease tumor development in mice by delaying early-phase cell cycle progression (45). Similarly, the present study shows that systemic nanoliposomal ceramide enhances sorafenib efficacy leading to cooperative tumor inhibition, which has therapeutic potential for more effectively treating melanoma and breast cancer.

In the past, the use of ceramide as a therapeutic agent has been limited by cell impermeability, precipitation in aqueous solutions, use of non–Food and Drug Administration-approved excipients, or circulatory metabolism into promitogenic products (22, 23, 29–32). In this study, ceramide was loaded into nanoliposomal delivery vehicles that can be used alone to deliver systemic exogenous ceramide or in conjunction with chemotherapeutics, such as sorafenib (22, 23, 29, 30). These nanoliposomes are 80 ± 15 nm in size and contain 30 mol% cell-permeable ceramide (23). The LD_{50} dose of nanoliposomal ceramide is ~100 mg/kg, which is

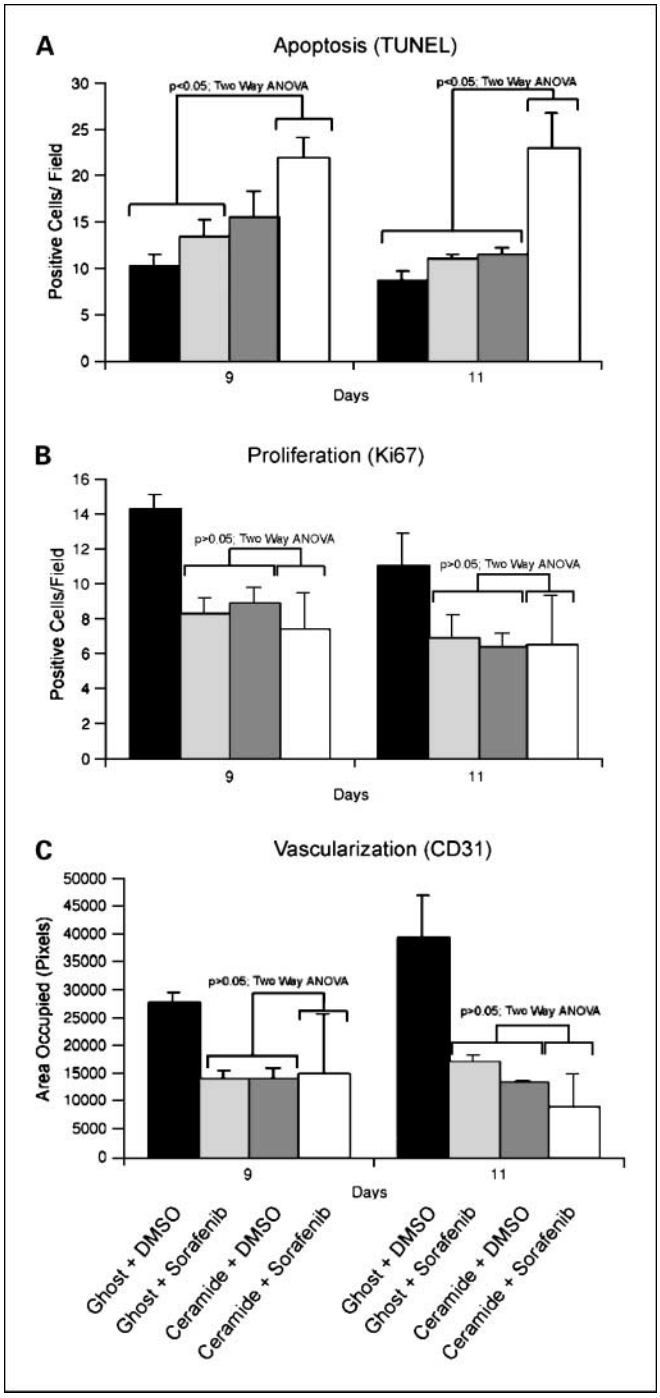

Fig. 6. Sorafenib and nanoliposomal ceramide combination therapy enhances tumor cell apoptosis. Size- and time-matched melanoma (UACC 903) tumors treated with sorafenib + nanoliposomal ceramide were compared with ghost liposomes + sorafenib, nanoliposomal ceramide + DMSO, and ghost liposomes + DMSO. Levels of cellular apoptosis, proliferation, or vascular development were quantified. *A,* statistically significant higher apoptosis levels were observed in tumors treated with nanoliposomal ceramide + sorafenib compared with vehicle- or monotherapy-treated cells at days 9 and 11 ($P < 0.05$, two-way ANOVA). *B,* decreased proliferation was observed in all groups at days 9 and 11 compared with the ghost liposomes + DMSO control – treated tumors ($P < 0.05$, two-way ANOVA). However, no significant differences were observed between individual and combined treatment regimens ($P > 0.05$, two-way ANOVA). *C,* although treatment regimens decreased vascular development in tumors, no significant change in vascularization was observed when comparing tumors treated with ceramide and sorafenib with those exposed to single agents ($P > 0.05$, two-way ANOVA).

~4-fold higher than doses used in this study (22). Furthermore, ceramide liposomes selectively kill cancer cells in animal tumors, likely due to accumulation caused by the leaky tumor vasculature (46). Nanoliposomal ceramide mediates apoptosis primarily by inactivation of Akt, which restores cancer cell apoptotic sensitivity, making them receptive to killing via chemotherapeutic agents such as sorafenib (23, 47–49).

Combining sorafenib and nanoliposomal ceramide decreased MAPK and PI3K/Akt signaling, which enhanced apoptosis causing cooperative tumor inhibition. Mechanistically, nanoliposomal ceramide reduced pAkt levels and sensitized cancer cells to apoptosis mediated by sorafenib, thereby effectively killing breast cancer and melanoma cells. Combining sorafenib and nanoliposomal ceramide led to synergistic cooperation between agents in cultured cells and enhanced tumor-inhibitory effectiveness. Furthermore, no significant weight loss, changes in liver morphology, or increases in blood variables indicating systemic toxicity was observed in animals, suggesting negligible systemic toxicity.

Mechanistically, tumor inhibition by combining sorafenib and nanoliposomal ceramide was due to increased apoptosis compared with single agents. Sorafenib has previously been shown to inhibit angiogenesis with decreased proliferation and increased apoptosis being secondary effects (11). In this study, combining sorafenib and nanoliposomal ceramide decreased levels of angiogenesis and proliferation in animal tumors to levels similar to those of the individual agents. In contrast, the combination had a significant effect on tumor cell apoptosis. These results contradict experiments on cultured cells, which showed the combination affected rates of both proliferation and apoptosis. Discrepancies of this type between cell culture and animal studies are common, necessitating pharmacologic agents be tested in animal models and not solely on cultured cells to evaluate efficacy and mechanistic basis for inhibition (50). In conclusion, combining sorafenib with nanoliposomal ceramide has significant therapeutic potential for melanoma and breast cancer patients by significantly increasing cancer cell apoptosis compared with each agent alone.

In conclusion, this study shows that therapeutically targeting the MAPK and PI3K/Akt pathways using sorafenib and nanoliposomal ceramide led to more effective cancer cell inhibition than either single agent alone. The combination synergistically enhanced the antiproliferative actions of sorafenib, which promoted cellular apoptosis in both cultured cells and tumors, with potential to more effectively inhibit melanoma and breast cancer in patients. Thus, this study establishes the foundation for clinical trials evaluating the efficacy of combining sorafenib with nanoliposomal ceramide for treatment of melanoma and breast cancer patients.

Disclosure of Potential Conflicts of Interest

M. Kester: Keystone Nano, Inc. and TRACON Pharmaceuticals. The other authors disclosed no potential conflicts of interest.

Acknowledgments

We thank Dr. Arati Sharma and James Kaiser for technical assistance.

References

1. Hanahan D, Weinberg RA. The hallmarks of cancer. Cell 2000;100:57–70.
2. Chang F, Steelman LS, Shelton JG, et al. Regulation of cell cycle progression and apoptosis by the Ras/Raf/MEK/ERK pathway [review]. Int J Oncol 2003;22:469–80.
3. Altomare DA, Testa JR. Perturbations of the AKT signaling pathway in human cancer. Oncogene 2005;24:7455–64.
4. Smalley KS. A pivotal role for ERK in the oncogenic behaviour of malignant melanoma? Int J Cancer 2003;104:527–32.
5. Mercer KE, Pritchard CA. Raf proteins and cancer: B-Raf is identified as a mutational target. Biochim Biophys Acta 2003;1653:25–40.
6. Brose MS, Volpe P, Feldman M, et al. BRAF and RAS mutations in human lung cancer and melanoma. Cancer Res 2002;62:6997–7000.
7. Davies H, Bignell GR, Cox C, et al. Mutations of the BRAF gene in human cancer. Nature 2002;417:949–54.
8. Yazdi AS, Palmedo G, Flaig MJ, et al. Mutations of the BRAF gene in benign and malignant melanocytic lesions. J Invest Dermatol 2003;121:1160–2.
9. Miller CJ, Cheung M, Sharma A, et al. Method of mutation analysis may contribute to discrepancies in reports of (V599E) BRAF mutation frequencies in melanocytic neoplasms. J Invest Dermatol 2004;123:990–2.
10. Maemura M, Iino Y, Koibuchi Y, Yokoe T, Morishita Y. Mitogen-activated protein kinase cascade in breast cancer. Oncology 1999;57 Suppl 2:37–44.
11. Sharma A, Trivedi NR, Zimmerman MA, Tuveson DA, Smith CD, Robertson GP. Mutant V599EB-Raf regulates growth and vascular development of malignant melanoma tumors. Cancer Res 2005;65:2412–21.
12. Sumimoto H, Miyagishi M, Miyoshi H, et al. Inhibition of growth and invasive ability of melanoma by inactivation of mutated BRAF with lentivirus-mediated RNA interference. Oncogene 2004;23:6031–9.
13. Hingorani SR, Jacobetz MA, Robertson GP, Herlyn M, Tuveson DA. Suppression of BRAF(V599E) in human melanoma abrogates transformation. Cancer Res 2003;63:5198–202.
14. Wilhelm SM, Carter C, Tang L, et al. BAY 43-9006 exhibits broad spectrum oral antitumor activity and targets the RAF/MEK/ERK pathway and receptor tyrosine kinases involved in tumor progression and angiogenesis. Cancer Res 2004;64:7099–109.
15. Wilhelm S, Carter C, Lynch M, et al. Discovery and development of sorafenib: a multikinase inhibitor for treating cancer. Nat Rev Drug Discov 2006;5:835–44.
16. Eisen T, Ahmad T, Flaherty KT, et al. Sorafenib in advanced melanoma: a phase II randomised discontinuation trial analysis. Br J Cancer 2006;95:581–6.
17. Kane RC, Farrell AT, Saber H, et al. Sorafenib for the treatment of advanced renal cell carcinoma. Clin Cancer Res 2006;12:7271–8.
18. Toker A, Yoeli-Lerner M. Akt signaling and cancer: surviving but not moving on. Cancer Res 2006;66:3963–6.
19. Madhunapantula SV, Sharma A, Robertson GP. PRAS40 deregulates apoptosis in malignant melanoma. Cancer Res 2007;67:3626–36.
20. Simstein R, Burow M, Parker A, Weldon C, Beckman B. Apoptosis, chemoresistance, and breast cancer: insights from the MCF-7 cell model system. Exp Biol Med (Maywood) 2003;228:995–1003.
21. Stahl JM, Sharma A, Cheung M, et al. Deregulated Akt3 activity promotes development of malignant melanoma. Cancer Res 2004;64:7002–10.
22. Stover TC, Sharma A, Robertson GP, Kester M. Systemic delivery of liposomal short-chain ceramide limits solid tumor growth in murine models of breast adenocarcinoma. Clin Cancer Res 2005;11:3465–74.
23. Stover T, Kester M. Liposomal delivery enhances short-chain ceramide-induced apoptosis of breast cancer cells. J Pharmacol Exp Ther 2003;307:468–75.
24. Yang L, Dan HC, Sun M, et al. Akt/protein kinase B signaling inhibitor-2, a selective small molecule inhibitor of Akt signaling with antitumor activity in cancer cells overexpressing Akt. Cancer Res 2004;64:4394–9.
25. Kolesnick RN, Kronke M. Regulation of ceramide production and apoptosis. Annu Rev Physiol 1998;60:643–65.
26. Hannun YA. The sphingomyelin cycle and the second messenger function of ceramide. J Biol Chem 1994;269:3125–8.
27. Spiegel S, Merrill AH, Jr. Sphingolipid metabolism and cell growth regulation. FASEB J 1996;10:1388–97.
28. Merrill AH, Jr., Schmelz EM, Dillehay DL, et al. Sphingolipids—the enigmatic lipid class: biochemistry, physiology, and pathophysiology. Toxicol Appl Pharmacol 1997;142:208–25.
29. Shabbits JA, Mayer LD. Intracellular delivery of ceramide lipids via liposomes enhances apoptosis *in vitro*. Biochim Biophys Acta 2003;1612:98–106.
30. Shabbits JA, Mayer LD. High ceramide content liposomes with *in vivo* antitumor activity. Anticancer Res 2003;23:3663–9.
31. Mehta S, Blackinton D, Omar I, et al. Combined

cytotoxic action of paclitaxel and ceramide against the human Tu138 head and neck squamous carcinoma cell line. Cancer Chemother Pharmacol 2000;46:85–92.

32. Han WS, Yoo JY, Youn SW, et al. Effects of C2-ceramide on the Malme-3M melanoma cell line. J Dermatol Sci 2002;30:10–9.

33. Stahl JM, Cheung M, Sharma A, Trivedi NR, Shanmugam S, Robertson GP. Loss of PTEN promotes tumor development in malignant melanoma. Cancer Res 2003;63:2881–90.

34. Chou TC, Talalay P. Quantitative analysis of dose-effect relationships: the combined effects of multiple drugs or enzyme inhibitors. Adv Enzyme Regul 1984;22:27–55.

35. Moore M, Hirte HW, Siu L, et al. Phase I study to determine the safety and pharmacokinetics of the novel Raf kinase and VEGFR inhibitor BAY 43-9006, administered for 28 days on/7 days off in patients with advanced, refractory solid tumors. Ann Oncol 2005;16:1688–94.

36. Jane EP, Premkumar DR, Pollack IF. Coadministration of sorafenib with rottlerin potently inhibits cell proliferation and migration in human malignant glioma cells. J Pharmacol Exp Ther 2006;319:1070–80.

37. Smalley KS, Haass NK, Brafford PA, Lioni M, Flaherty KT, Herlyn M. Multiple signaling pathways must be targeted to overcome drug resistance in cell lines derived from melanoma metastases. Mol Cancer Ther 2006;5:1136–44.

38. Yu C, Friday BB, Lai JP, et al. Cytotoxic synergy between the multikinase inhibitor sorafenib and the proteasome inhibitor bortezomib *in vitro*: induction of apoptosis through Akt and c-Jun NH_2-terminal kinase pathways. Mol Cancer Ther 2006;5:2378–87.

39. Siu LL, Awada A, Takimoto CH, et al. Phase I trial of sorafenib and gemcitabine in advanced solid tumors with an expanded cohort in advanced pancreatic cancer. Clin Cancer Res 2006;12:144–51.

40. Bedogni B, O'Neill MS, Welford SM, et al. Topical treatment with inhibitors of the phosphatidylinositol 3′-kinase/Akt and Raf/mitogen-activated protein kinase kinase/extracellular signal-regulated kinase pathways reduces melanoma development in severe combined immunodeficient mice. Cancer Res 2004;64:2552–60.

41. Abou-Alfa GK, Schwartz L, Ricci S, et al. Phase II study of sorafenib in patients with advanced hepatocellular carcinoma. J Clin Oncol 2006;24:4293–300.

42. Ratain MJ, Eisen T, Stadler WM, et al. Phase II placebo-controlled randomized discontinuation trial of sorafenib in patients with metastatic renal cell carcinoma. J Clin Oncol 2006;24:2505–12.

43. Richly H, Henning BF, Kupsch P, et al. Results of a phase I trial of sorafenib (BAY 43-9006) in combination with doxorubicin in patients with refractory solid tumors. Ann Oncol 2006;17:866–73.

44. Richly H, Kupsch P, Passage K, et al. Results of a phase I trial of BAY 43-9006 in combination with doxorubicin in patients with primary hepatic cancer. Int J Clin Pharmacol Ther 2004;42:650–1.

45. Plastaras JP, Kim SH, Liu YY, et al. Cell cycle-dependent and schedule-dependent antitumor effects of sorafenib combined with radiation. Cancer Res 2007;67:9443–54.

46. McDonald DM, Baluk P. Significance of blood vessel leakiness in cancer. Cancer Res 2002;62:5381–5.

47. Zhou H, Summers SA, Birnbaum MJ, Pittman RN. Inhibition of Akt kinase by cell-permeable ceramide and its implications for ceramide-induced apoptosis. J Biol Chem 1998;273:16568–75.

48. Martin D, Salinas M, Fujita N, Tsuruo T, Cuadrado A. Ceramide and reactive oxygen species generated by H_2O_2 induce caspase-3-independent degradation of Akt/protein kinase B. J Biol Chem 2002;277:42943–52.

49. Kim DS, Kim SY, Moon SJ, et al. Ceramide inhibits cell proliferation through Akt/PKB inactivation and decreases melanin synthesis in Mel-Ab cells. Pigment Cell Res 2001;14:110–5.

50. Madhunapantula SV, Robertson GP. Is B-Raf a good therapeutic target for melanoma and other malignancies? Cancer Res 2008;68:5–8.